

Supporting Information: Dynamics of Poly(ethylene oxide)-capped Gold Nanoparticles in aqueous solution studied by neutron spin echo spectroscopy

Alessio De Francesco,^{a)} Luisa Scaccia,^{b)} R. Bruce Lennox,^{c)} Eleonora Guarini,^{d)} Ubaldo Bafile,^{e)} Peter Falus,^{f)} and Marco Maccarini^{g)}

I. COHERENT AND INCOHERENT SCATTERING

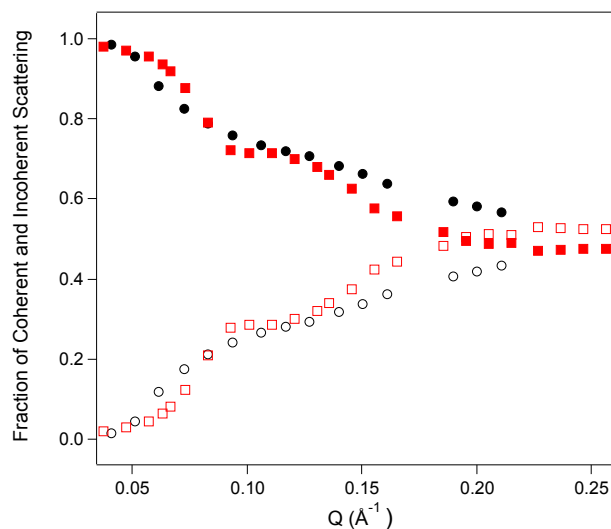


Figure S 1. Fractions of coherent (filled symbols) and incoherent (empty symbols) contributions to the NSE signal measured for PEG2000 AuNP (black circles) and PEG400 AuNP (red squares).

^{a)} Consiglio Nazionale delle Ricerche, Istituto Officina dei Materiali c/o OGG Grenoble, France

^{b)} Dipartimento di Economia e Diritto, Università di Macerata, Via Crescimbeni 20, 62100 Macerata, Italy

^{c)} Dep. Chemistry, McGill University, Sherbrooke St. West, Montreal, Canada

^{d)} Dipartimento di Fisica e Astronomia, Università di Firenze, via G. Sansone 1, I-50019 Sesto Fiorentino, Italy

^{e)} Consiglio Nazionale delle Ricerche, Istituto di Fisica Applicata "Nello Carrara", via Madonna del Piano 10, I-50019 Sesto Fiorentino, Italy

^{f)} Institut Laue-Langevin, Grenoble, France

^{g)} Université Grenoble Alpes - Laboratoire TIMC/IMAG UMR CNRS 5525 Grenoble, France; Electronic mail: marco.maccarini@univ-grenoble-alpes.fr

II. PEG2000 AUNP

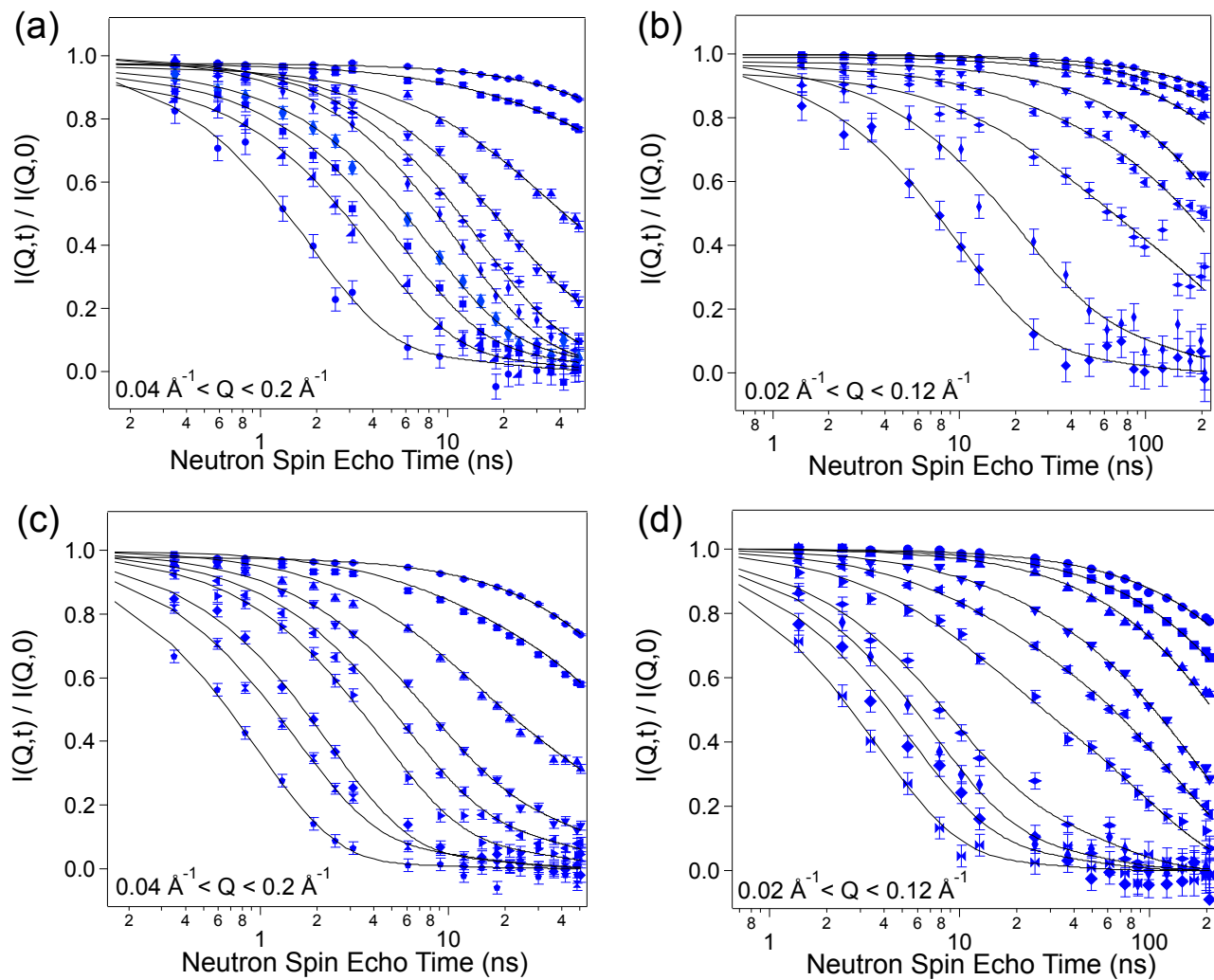


Figure S 2. NSE curves representing $I(Q,t)/I(Q,0)$ measured for PEG2000 AuNP dispersed in D_2O at different temperatures and wavelengths. (a) $\lambda = 10 \text{ \AA}$, $T = 280 \text{ K}$; (b) $\lambda = 16 \text{ \AA}$, $T = 280 \text{ K}$; (c) $\lambda = 10 \text{ \AA}$, $T = 318 \text{ K}$; (d) $\lambda = 16 \text{ \AA}$, $T = 318 \text{ K}$. The Q values increase from above to bottom.

Q [\AA^{-1}]	A_1	τ_D [ns]	τ_{pol} [ns]	k	P($k y$)	D_T [$\text{\AA}^2\text{ns}^{-1}$]
0.04	1	430 ± 10		1	0.82	1.42 ± 0.06
0.05	0.93 ± 0.02	300 ± 10	16 ± 5	2	1	1.28 ± 0.07
0.06	0.54 ± 0.05	200 ± 20	24 ± 5	2	1	1.3 ± 0.1
0.07	0.25 ± 0.04	150 ± 10	18 ± 2	2	0.51	1.3 ± 0.1
0.08	0.10 ± 0.03	110 ± 10	15 ± 0.7	2	1	1.3 ± 0.1
0.09	0.07 ± 0.02	89 ± 6	11.7 ± 0.6	2	0.56	1.3 ± 0.1
0.11	0.05 ± 0.02	69 ± 7	9.5 ± 0.5	2	0.69	1.3 ± 0.1
0.12	0.10 ± 0.3	56 ± 6	7.8 ± 0.5	2	0.72	1.3 ± 0.1
0.13	0.11 ± 0.3	48 ± 5	6.3 ± 0.5	2	0.73	1.3 ± 0.1
0.14	0.10 ± 0.04	39 ± 4	5.6 ± 0.7	2	0.72	1.3 ± 0.1
0.15	0.09 ± 0.03	34 ± 3	4.6 ± 0.5	2	0.86	1.3 ± 0.1
0.16	0.08 ± 0.02	29 ± 2	4 ± 0.2	2	0.83	1.3 ± 0.1
0.19	0.06 ± 0.02	21 ± 2	2.3 ± 0.2	2	0.93	1.3 ± 0.1
0.20	0.06 ± 0.02	19 ± 2	2.0 ± 0.1	2	0.93	1.3 ± 0.1
0.21	0.07 ± 0.04	17 ± 2	1.8 ± 0.2	2	0.94	1.3 ± 0.1

Table S I. Fitting parameters obtained for the NSE measurements taken on the PEG2000 AuNP at 280 K and at $\lambda = 10 \text{ \AA}$. P($k|y$) is the probability for the most frequently chosen model. The constant γ (that was not reported in this table and in the next ones) in front of Eq. 23 in the manuscript, resulted always in the range 0.98–1 with few exceptions within a 5% difference from 1.

Q [\AA^{-1}]	A_1	τ_D [ns]	τ_{pol} [ns]	k	P($k y$)	D_T [$\text{\AA}^2\text{ns}^{-1}$]
0.019	1	1890 ± 50		1	0.98	1.41 ± 0.04
0.026	1	1250 ± 40		1	0.97	1.18 ± 0.04
0.032	1	860 ± 40		1	0.87	1.11 ± 0.05
0.044	1	400 ± 10		1	0.79	1.29 ± 0.04
0.050	0.90 ± 0.02	310 ± 7	20 ± 7	2	0.91	1.30 ± 0.03
0.057	0.66 ± 0.04	230 ± 10	28 ± 9	2	0.59	1.31 ± 0.07
0.076	0.22 ± 0.06	132 ± 7	20 ± 4	2	0.55	1.32 ± 0.07
0.082	0.09 ± 0.04	111 ± 6	16 ± 2	2	0.74	1.32 ± 0.07
0.089	0.19 ± 0.05	96 ± 5	13 ± 2	2	0.68	1.32 ± 0.07
0.110	0.10 ± 0.04	62 ± 3	9.7 ± 0.9	2	0.74	1.32 ± 0.07
0.116	0.13 ± 0.05	56 ± 3	9 ± 1	2	0.78	1.32 ± 0.07
0.123	0.22 ± 0.07	50 ± 3	8 ± 2	2	0.70	1.32 ± 0.07

Table S II. Fitting parameters obtained for the NSE measurements taken on the PEG2000 AuNP at 280K and at $\lambda = 16 \text{ \AA}$.

Q [\AA^{-1}]	A_1	τ_D [ns]	τ_{pol} [ns]	β_2	$P(\beta_2 = 1 k = 2)$	k	$P(k y)$	$D_T[\text{\AA}^2\text{ns}^{-1}]$
0.041	1	177 ± 2				1	0.80	3.42 ± 0.09
0.051	0.86 ± 0.02	128 ± 9	9 ± 2	1	1*	2	1	3.0 ± 0.2
0.062	0.55 ± 0.03	87 ± 9	10 ± 1	1	1*	2	1	3.1 ± 0.3
0.072	0.28 ± 0.02	60 ± 6	7.5 ± 0.3	1.000 ± 0.005	0.97	2	0.77	3.2 ± 0.3
0.083	0.18 ± 0.02	47 ± 5	5.6 ± 0.3	1	1*	2	1	3.2 ± 0.3
0.094	0.11 ± 0.02	36 ± 4	4.2 ± 0.2	1.000 ± 0.006	0.97	2	0.84	3.2 ± 0.3
0.106	0.04 ± 0.01	27 ± 3	3.1 ± 0.1	0.99 ± 0.02	0.83	2	0.98	3.3 ± 0.3
0.127	0.06 ± 0.02	19 ± 2	2.3 ± 0.1	0.999 ± 0.008	0.96	2	0.98	3.3 ± 0.3
0.140	0.08 ± 0.02	15 ± 2	1.8 ± 0.1	0.99 ± 0.03	0.86	2	0.98	3.4 ± 0.3
0.150	0.10 ± 0.03	13 ± 1	1.50 ± 0.09	0.99 ± 0.03	0.80	2	0.98	3.4 ± 0.3
0.161	0.07 ± 0.02	12 ± 2	1.30 ± 0.08	0.99 ± 0.02	0.91	2	0.98	3.3 ± 0.3
0.190	0.03 ± 0.02	8.5 ± 0.9	0.95 ± 0.05	0.99 ± 0.02	0.89	2	0.99	3.3 ± 0.3
0.200	0.04 ± 0.02	7.6 ± 0.8	0.84 ± 0.06	0.99 ± 0.02	0.91	2	0.99	3.3 ± 0.3
0.211	0.03 ± 0.02	6.9 ± 0.7	0.78 ± 0.06	0.99 ± 0.02	0.91	2	0.99	3.3 ± 0.3

Table S III. Fitting parameters obtained for the NSE measurements taken on the PEG2000 AuNP at 318 K and at $\lambda = 10 \text{ \AA}$. By way of example in the 5th and the 6th column of this table we report also the average estimated value of β_2 and the probability to have $\beta_2 = 1$ when the two component model is chosen.

* For these datasets we set $k = 2$, for consistency with the results obtained for the other data sets, even if the model with two components is not the one with the highest posterior. Moreover the joint posterior distribution (conditional on $k = 2$) is bimodal. The first maximum in the distribution corresponds to $\beta_2 = 1$ and values of the other parameters as given in the table. The second maximum corresponds to values of the parameters that are meaningless from a physical point of view. For example, at $Q = 0.051 \text{ \AA}^{-1}$, the second mode corresponds to $\beta_2 = 0.71$, $A_1 = 0.27$, $\tau_D = 131.12 \text{ ns}$ and $\tau_{pol} = 86.55 \text{ ns}$, i.e. values of the parameters completely incongruous with the trend observed for the other datasets. This second mode is probably a spurious solution, related to a local maximum and was, therefore, discarded. Thus, we simply set $\beta_2 = 1$ for these datasets, in analogy with the values estimated for the remaining datasets. In all the other datasets we reported in the table the average value of β_2 when $k = 2$ as estimated by the algorithm but a value of 1 for the stretching coefficient when the conditional probability $P(\beta_2 = 1|k = 2) > 0.5$ was adopted for the final curve fitting.

Q [\AA^{-1}]	A_1	τ_D [ns]	τ_{pol} [ns]	k	$P(k y)$	$D_T[\text{\AA}^2\text{ns}^{-1}]$
0.019	1	760 ± 10		1	0.76	3.5 ± 0.2
0.026	1	488 ± 4		1	0.58	3.2 ± 0.3
0.032	1	312 ± 4		1	0.75	3.0 ± 0.1
0.044	0.92 ± 0.02	175 ± 6	16 ± 5	2	1*	3.1 ± 0.3
0.051	0.80 ± 0.02	135 ± 5	12 ± 2	2	1*	3.1 ± 0.3
0.057	0.64 ± 0.04	92 ± 7	10 ± 2	2	1*	3.4 ± 0.3
0.076	0.28 ± 0.06	52 ± 5	8 ± 1	2	0.92	3.4 ± 0.3
0.082	0.14 ± 0.05	46 ± 5	7.1 ± 0.6	2	0.93	3.3 ± 0.3
0.089	0.10 ± 0.04	38 ± 4	5.3 ± 0.6	2	0.97	3.4 ± 0.3
0.110	0.06 ± 0.03	26 ± 3	3.6 ± 0.2	2	0.94	3.2 ± 0.2
0.116	0.11 ± 0.04	23 ± 2	3.1 ± 0.3	2	0.97	3.3 ± 0.3
0.123	0.10 ± 0.04	21 ± 2	2.7 ± 0.3	2	0.85	3.2 ± 0.3

Table S IV. Fitting parameters obtained for the NSE measurements taken on the PEG2000 AuNP at 318 K and at $\lambda = 16 \text{ \AA}$. *Refer to note in Table III.

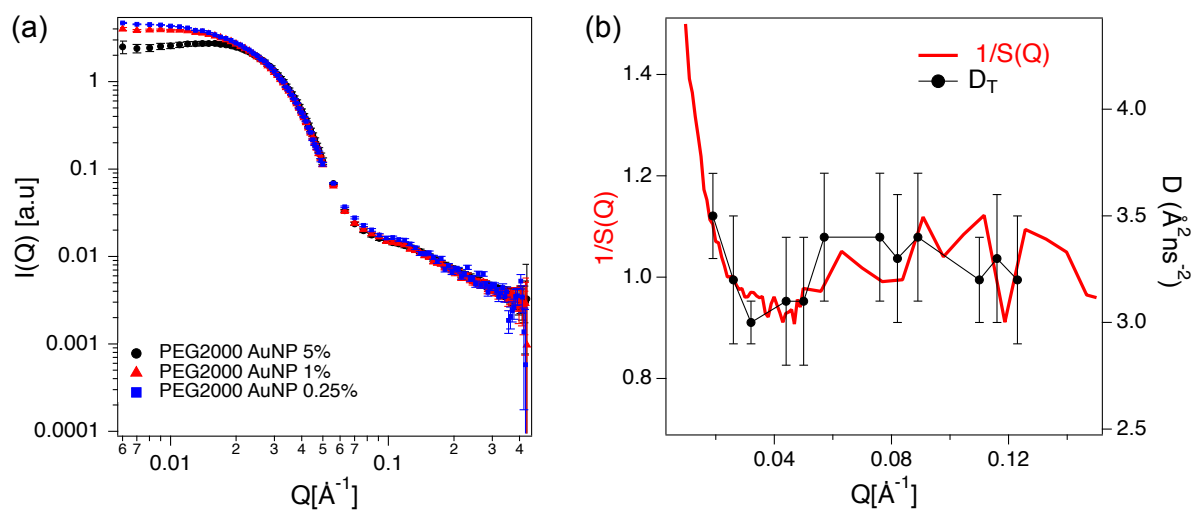


Figure S 3. (a) SANS curves normalised to the concentration of the PEG2000 Au NP. (b) Inverse of the structure factor ($1/S(Q)$) extracted from the SANS curves at different concentrations and the translational diffusion D obtained by the Bayesian analysis.

III. PEG400 AUNP

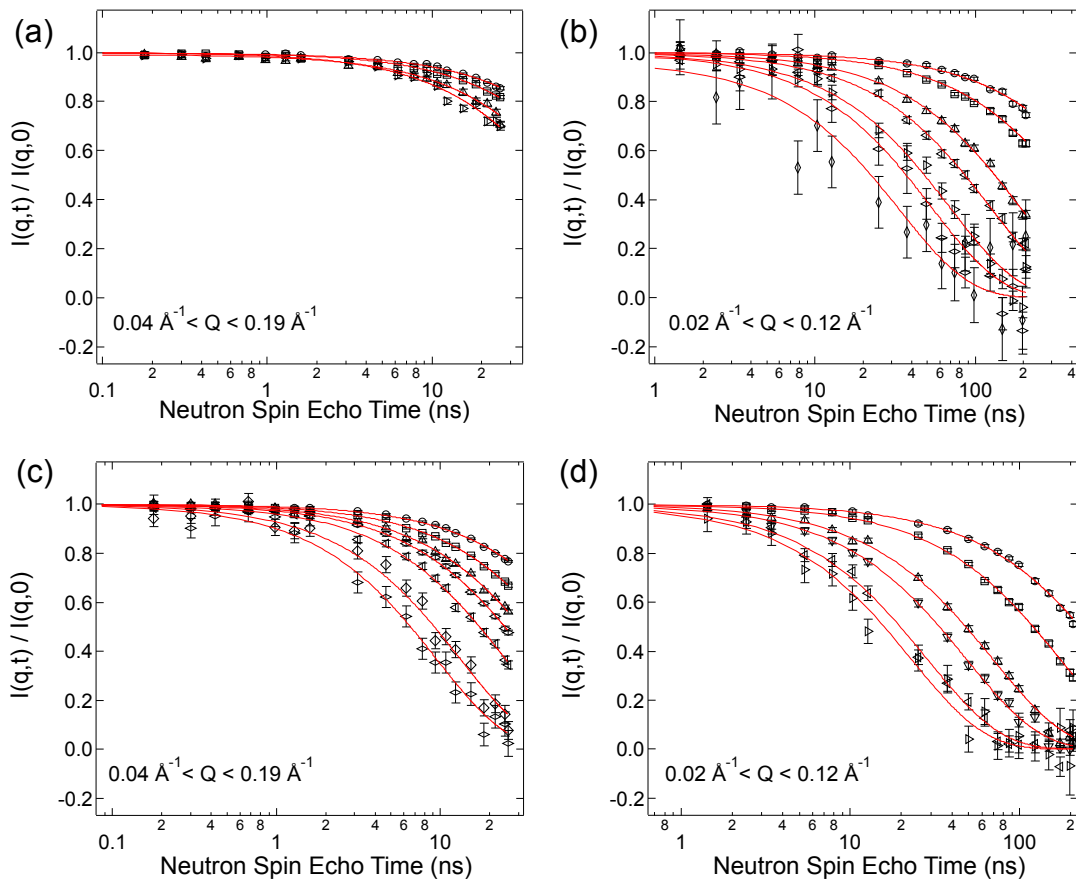


Figure S 4. NSE curves representing $I(Q, t)/I(Q, 0)$ measured on the PEG400 AuNP at different temperatures and wavelengths. (a) $\lambda = 8 \text{ \AA}$, $T = 280 \text{ K}$; (b) $\lambda = 16 \text{ \AA}$, $T = 280 \text{ K}$; (c) $\lambda = 8 \text{ \AA}$, $T = 318 \text{ K}$ (d) $\lambda = 16 \text{ \AA}$, $T = 318 \text{ K}$. The Q values increase from above to bottom. The red solid lines represent the best fit to the data.

$Q [\text{\AA}^{-1}]$	A_1	$\tau_D [\text{ns}]$	k	$P(k y)$	$D_T [\text{\AA}^2 \text{ns}^{-1}]$
0.047	1	173 ± 7	1	0.69	2.6 ± 0.2
0.057	1	128 ± 5	1	0.35*	2.4 ± 0.2
0.067	1	90 ± 3	1	0.57	2.4 ± 0.2
0.063	1	93 ± 3	1	0.83	2.6 ± 0.3
0.073	1	71 ± 2	1	0.84	2.6 ± 0.2
0.083	1	58 ± 5	1	0.59	2.6 ± 0.3
0.093	1	42 ± 5	1	0.79	2.4 ± 0.3

Table S V. Fitting parameters obtained for the NSE measurements on the PEG400 AuNP taken at 280 K and at $\lambda = 8 \text{ \AA}$.

* For this particular dataset the data are scarcely informative about the number of components and the algorithm assigns relevant posterior probabilities to models with either 1, 2 or 3 components. Therefore, in this case, model choice takes advantage from results obtained for similar data sets, for which the posterior distribution of the number of components is more peaked and the model with 1 component is largely supported.

Q [\AA^{-1}]	A_1	τ_D [ns]	k	P(k y)	$D_T[\text{\AA}^2\text{ns}^{-1}]$
0.02	1	800 ± 20	1	0.89	3.1 ± 0.1
0.03	1	458 ± 9	1	0.59	2.5 ± 0.1
0.05	1	191 ± 3	1	0.78	2.5 ± 0.1
0.06	1	124 ± 2	1	0.71	2.4 ± 0.3
0.07	1	69 ± 3	1	0.91	2.7 ± 0.3
0.08	1	54 ± 4	1	0.92	2.7 ± 0.2
0.11	1	34 ± 5	1	0.69	2.4 ± 0.4

Table S VI. Fitting parameters obtained for the NSE measurements on the PEG400 AuNP taken at 280 K and at $\lambda = 16 \text{ \AA}$.

Q [\AA^{-1}]	A_1	τ_D [ns]	k	P(k y)	$D_T[\text{\AA}^2\text{ns}^{-1}]$
0.02	1	800 ± 20	1	0.89	3.1 ± 0.1
0.037	1	99 ± 1	1	0.87	7.2 ± 0.4
0.048	1	64.4 ± 0.8	1	0.89	6.8 ± 0.4
0.057	1	44.7 ± 0.6	1	0.91	6.8 ± 0.5
0.067	1	31.6 ± 0.5	1	0.95	7.1 ± 0.2
0.063	1	35.7 ± 0.4	1	0.94	7.0 ± 0.1
0.073	1	25.0 ± 0.4	1	0.96	7.5 ± 0.3
0.083	1	19.3 ± 0.5	1	0.91	7.6 ± 0.6
0.093	1	17.1 ± 0.7	1	0.90	6.9 ± 0.4
0.100	1	15.0 ± 0.5	1	0.92	6.6 ± 0.3
0.111	1	13.2 ± 0.5	1	0.96	6.2 ± 0.3
0.121	1	10.8 ± 0.4	1	0.97	6.4 ± 0.3
0.131	1	9.5 ± 0.4	1	0.96	6.2 ± 0.3
0.136	1	8.7 ± 0.4	1	0.94	6.2 ± 0.5
0.146	1	7.5 ± 0.4	1	0.96	6.3 ± 0.3
0.155	1	8.3 ± 0.9	1	0.83	5.3 ± 0.6
0.165	1	6.6 ± 0.9	1	0.92	5.6 ± 0.7
0.186	1	4.7 ± 0.8	1	0.93	6 ± 1

Table S VII. Fitting parameters obtained for the NSE measurements on the PEG400 AuNP taken at 318 K and at $\lambda = 8 \text{ \AA}$.

Q [\AA^{-1}]	A_1	τ_D [ns]	k	P(k y)	$D_T[\text{\AA}^2\text{ns}^{-1}]$
0.02	1	800 ± 20	1	0.89	3.1 ± 0.1
0.02	1	329 ± 4	1	0.74	7.6 ± 0.2
0.03	1	173 ± 2	1	0.87	6.6 ± 0.4
0.05	1	69 ± 1	1	0.94	6.8 ± 0.3
0.06	1	48 ± 1	1	0.93	6.6 ± 0.2
0.07	1	28 ± 1	1	0.94	6.7 ± 0.3
0.08	1	23 ± 2	1	0.85	6.5 ± 0.6
0.11	1	12 ± 2	1	0.86	6.8 ± 0.8
0.12	1	10 ± 2	1	0.87	6.7 ± 0.9

Table S VIII. Fitting parameters obtained for the NSE measurements on the PEG400 AuNP taken at 318 K and at $\lambda = 16 \text{ \AA}$.

IV. PEG2000

Q [\AA^{-1}]	A_1	τ_1 [ns]	τ_2 [ns]	k	P($k y$)
0.06	1	24.3 ± 0.4		1	0.75
0.08	1	17.7 ± 0.2		1	0.65
0.09	0.5 ± 0.2	9 ± 2	23 ± 7	2	0.64
0.1	0.6 ± 0.2	7 ± 2	20 ± 5	2	0.64
0.12	0.6 ± 0.2	6 ± 1	16 ± 4	2	0.65
0.13	0.6 ± 0.2	4.9 ± 0.9	12 ± 3	2	0.63
0.14	0.5 ± 0.2	3.7 ± 0.8	10 ± 2	2	0.61
0.15	0.4 ± 0.1	2.8 ± 0.6	7.5 ± 0.9	2	0.62
0.16	0.4 ± 0.2	2.3 ± 0.6	6 ± 1	2	0.57
0.19	0.5 ± 0.2	1.8 ± 0.3	5 ± 1	2	0.63
0.2	0.5 ± 0.1	1.8 ± 0.3	5.3 ± 0.8	2	0.61
0.21	0.6 ± 0.1	1.7 ± 0.2	6 ± 1	2	0.61
0.23	0.69 ± 0.07	1.6 ± 0.2	5 ± 1	2	0.66
0.24	0.7 ± 0.1	1.6 ± 0.2	5 ± 1	2	0.67
0.25	0.69 ± 0.05	1.11 ± 0.09	6 ± 2	2	0.73

Table S IX. Fitting parameters obtained for the NSE measurements on the PEG2000 in D_2O at concentration of 10% in weight taken at 280 K and at $\lambda = 8 \text{ \AA}$.

Q [\AA^{-1}]	A_1	τ_1 [ns]	τ_2 [ns]	k	P($k y$)
0.06	1	10.7 ± 0.1		1	0.55
0.08	0.5 ± 0.2	5 ± 1	11 ± 2	2	0.64
0.09	0.5 ± 0.2	3.8 ± 0.9	7 ± 1	2	0.63
0.1	0.7 ± 0.1	3.3 ± 0.3	8.5 ± 3	2	0.68
0.12	0.6 ± 0.2	2.3 ± 0.4	4.8 ± 0.9	2	0.72
0.13	0.7 ± 0.1	1.9 ± 0.2	5 ± 1	2	0.73
0.14	0.7 ± 0.2	1.7 ± 0.2	3.6 ± 0.9	2	0.78
0.15	0.7 ± 0.1	1.3 ± 0.2	3.6 ± 0.9	2	0.81
0.16	0.8 ± 0.1	1.2 ± 0.1	3.5 ± 0.2	2	0.81
0.19	0.7 ± 0.2	0.9 ± 0.1	2.1 ± 0.6	2	0.75
0.2	0.90 ± 0.05	0.89 ± 0.02	-	2	0.82
0.21	0.97 ± 0.03	0.73 ± 0.04	-	1	0.53
0.23	0.93 ± 0.05	0.64 ± 0.02	-	2	0.85
0.24	0.95 ± 0.05	0.52 ± 0.02	-	2	0.91
0.25	0.94 ± 0.05	0.44 ± 0.02	-	2	0.93

Table S X. Fitting parameters obtained for the NSE measurements on the PEG2000 in D_2O at concentration of 10% in weight taken at 318 K and at $\lambda = 8 \text{ \AA}$.

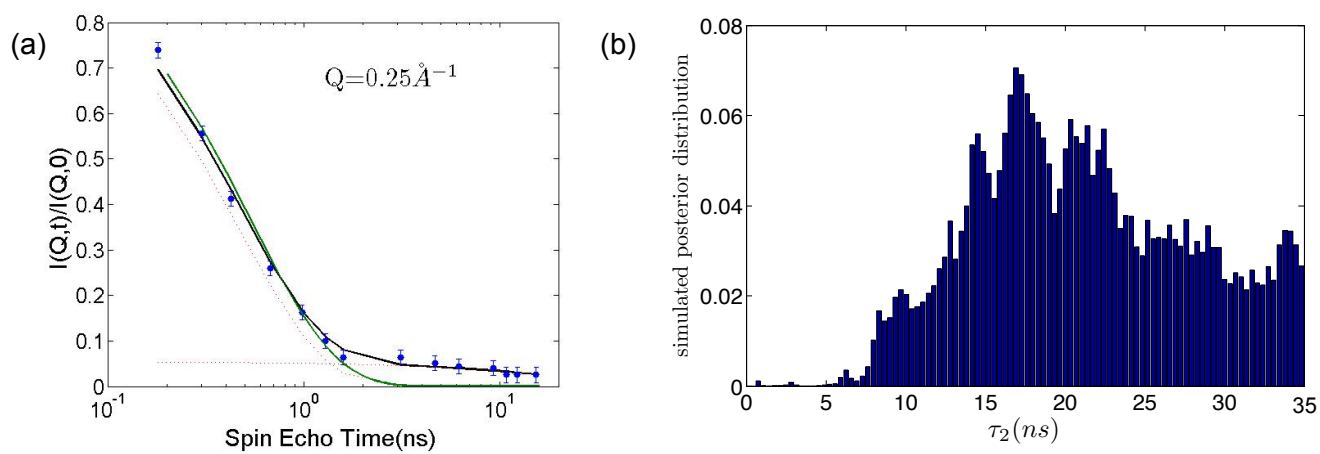


Figure S 5. (a) NSE curves representing $I(Q,t)/I(Q,0)$ measured on the PEG2000 at 318 K, $\lambda = 8 \text{ \AA}$, $Q = 0.25 \text{ \AA}^{-1}$ (symbols). The lines represent the best fits for the models with one (green continuous line) and two (dash black line) components; the dotted lines are the two contributions plotted separately corresponding to the model with two components. (b) Posterior distribution of the τ_2 obtained by the Bayesian analysis.

V. PEG400

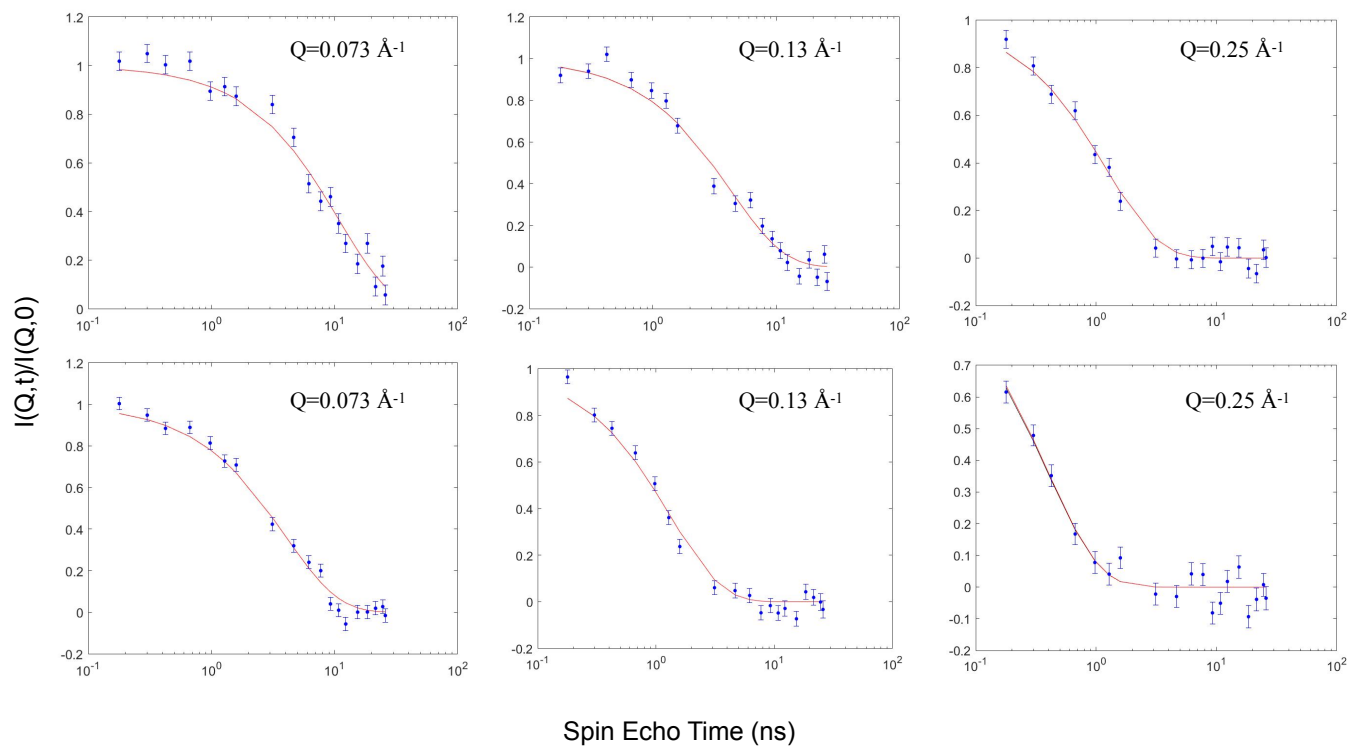


Figure S 6. NSE curves representing $I(Q,t)/I(Q,0)$ measured on the PEG400 homopolymer 5% concentration, at 280 K (top panels) and 318 K (bottom panels) at three selected Q values and $\lambda=8$ Å. The best fit curves (red continuous line) are shown.

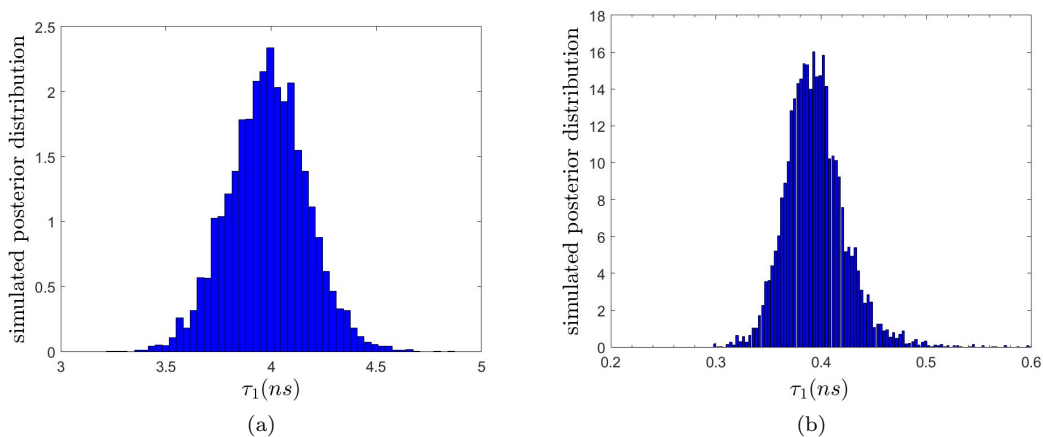


Figure S 7. Two examples of the posterior distribution function of τ_1 for the PEG400 homopolymers at 318 K, $\lambda=8$ Å and $Q = 0.073$ Å⁻¹ (a) and $Q = 0.25$ Å⁻¹ (b).

VI. COMPLEMENTARY INFORMATION TO THE BAYESIAN ANALYSIS

A. *The RJ-MCMC algorithm

The RJ-MCMC sampler we propose performs M sweeps and, at each sweep m , all the parameters, including k , are updated in turn. This is performed by drawing the new values of a certain parameter conditionally on the data and all the other parameters. The algorithm uses different fixed-dimension moves to update the model parameters, conditionally on a fixed k , plus a variable dimension move to update the number of components k .

In the fixed dimension moves, all the parameters, but ν , are updated by means of Metropolis-Hastings moves¹. For a generic parameter θ to be updated, the Metropolis-Hastings move proposes, at each sweep m , a new candidate value θ' , drawn from a proposal distribution $q(\cdot|\theta)$, which depends on the current value of θ as well as from tuning parameters. This candidate value is then accepted with a probability calculated according to an acceptance rule, which ensures that the Markov chain converges to an equilibrium distribution which is the joint posterior of the parameters, and is given by $\min\{1, R\}$, where

$$R = \frac{P(y|\Theta') P(\Theta') q(\theta|\theta')}{P(y|\Theta) P(\Theta) q(\theta'|\theta)}, \quad (1)$$

with Θ' denoting the whole parameter vector, in which the parameter θ has been substituted by θ' , $P(y|\Theta)$ being the likelihood and $P(\Theta)$ the prior on the parameters. Notice that the product of the first two ratios is simply the ratio between the posteriors evaluated in Θ' and Θ , respectively, with the normalizing constants cancelling out. The tuning parameters are tuned during some pilot running of the chain in such a way to guarantee an acceptance rate of the Metropolis-Hastings move of approximately 30%. To give an example, we describe in detail the updating of the component weights A , the Metropolis-Hastings updating of the other parameters being similar. At the m -th sweep of the algorithm, in order to update the current parameter A , we draw a candidate A' from a proposal $q(A'|A)$. A reasonable and natural choice of the proposal distribution for A' is the Dirichlet distribution with vector of parameters proportional to the current value of A , i.e. $\mathcal{D}(\epsilon_A A_1, \dots, \epsilon_A A_k)$, where ϵ_A is a tuning parameter. Under this choice, the proposed A' fulfils the constraints $A'_j \geq 0, \forall j$, and $\sum_{j=1}^k A'_j = 1$, and the distribution of each A'_j is centred on the current A_j , with variance controlled by ϵ_A . After drawing A' , the acceptance probability is calculated as $\min\{1, R\}$, where, accordingly to Eq.(1),

$$R = \frac{\prod_{i=1}^n \phi\left(y_i; \gamma \sum_{j=1}^k A'_j \exp\left(-\left(\frac{t_i}{\tau_j}\right)^{\beta_j}\right), \nu \sigma_i^2\right)}{\prod_{i=1}^n \phi\left(y_i; \gamma \sum_{j=1}^k A_j \exp\left(-\left(\frac{t_i}{\tau_j}\right)^{\beta_j}\right), \nu \sigma_i^2\right)} \times \frac{d(A'; \lambda)}{d(A; \lambda)} \times \frac{d(A; \epsilon_A A')}{d(A'; \epsilon_A A)},$$

with the three ratios being, respectively, the likelihood, the prior and the proposal ratios in Eq.(1), and $d(\cdot; \lambda)$ representing the density of the $\mathcal{D}(\lambda)$ distribution evaluated in a specific point “ \cdot ”. Finally, to decide whether the move is accepted or not, a random number u is drawn from a Uniform distribution on the interval $[0; 1]$ and compared with $\min\{1, R\}$. If $u < \min\{1, R\}$, the move is accepted and A' becomes the new parameter vector, otherwise the move is rejected and the parameter vector stays unchanged.

The parameter ν is instead updated by means of Gibbs sampling. The prior of this parameter is, in fact, conjugated with the likelihood and this results in a closed form for its full conditional distribution (i.e. the posterior distribution of the parameter, given the data and the value of all the other parameters). Thus, a new value of the parameter ν can be directly draw from its full conditional distribution, i.e.

$$\nu^{-1} \sim \mathcal{G}\left(\iota + \frac{n}{2}, \varsigma + \frac{1}{2} \sum_{i=1}^n \frac{\left(y_i - \gamma \sum_{j=1}^k A_j \exp\left(-\left(\frac{t_i}{\tau_j}\right)^{\beta_j}\right)\right)^2}{\sigma_i^2}\right). \quad (2)$$

Finally, updating the value of k implies a change of dimensionality for the vectors of weights A , stretching parameters β and relaxation times τ . We accomplish this by introducing a RJ move, consisting in a random choice between the birth of a new component or the death of an existing one. The probabilities of the birth/death alternatives are b_k and $d_k = 1 - b_k$, respectively, and depend only on the current value of k . Of course, $d_1 = 0$ and $b_{k_{\max}} = 0$; otherwise we choose $b_k = d_k = 0.5$, for $k = 2, \dots, k_{\max} - 1$. The move starts with a random choice between birth and death, using probabilities b_k and d_k . For a birth, we let $k' = k^m + 1$ and we pick a position j' at random among $1, \dots, k'$, with probability $1/k'$ for the place to be occupied by the new component j' . Then, a weight for the new component

is drawn as $A'_{j'} \sim \mathcal{B}(1, k)$ and a new vector A' is obtained by rescaling the existing weights, using $A'_j = A_j(1 - A'_{j'})$. Also, values of $\tau'_{j'}$ and $\beta'_{j'}$ are drawn from their respective priors

$$\tau'_{j'} \sim \mathcal{U}(0, \tau_{\max}) \quad \text{and} \quad \beta'_{j'} \sim \zeta \mathcal{B}(\kappa, \psi) + (1 - \zeta) \delta_{\beta'_{j'}, 1}$$

and collocated in the j' -th place of vectors τ and β to give τ' and β' , respectively. The parameters ν and γ remain unchanged. The acceptance probability for the birth move is calculated as $\min(1, B)$, where, accordingly to the RJ rule

$$B = \frac{\prod_{i=1}^n \phi(y_i; f'(t_i), \nu \sigma_i^2)}{\prod_{i=1}^n \phi(y_i; f(t_i), \nu \sigma_i^2)} \times \frac{p(k')}{p(k)} \times \frac{d(A'; \lambda)}{d(A; \lambda)} \times \frac{d_{k'}}{b_k \text{be}(A'_{j'}; 1, k)} \times (1 - A'_{j'})^k \quad (3)$$

where the first three factors in the multiplication represent the likelihood ratio (with $f(t_i)$ and $f'(t_i)$ being the model function evaluated at the current parameter set and the new parameter set, respectively) and the prior ratios, the fourth factor is the proposal ratio (with $\text{be}(\cdot; 1, k)$ denoting the beta density evaluated in “.”) and the fifth factor is the Jacobian of the transformation from A to A' . Thus, the acceptance probability for the RJ move is obtained from the Metropolis-Hastings acceptance probability in Eq.(1) simply multiplying by the Jacobian of the transformation from the old to the new parameters. For a death move, a component is chosen at random among any existing one, the chosen component is deleted and the remaining weights are rescaled to sum to 1. The acceptance probabilities for a death move is $D = \min(1, B^{-1})$, with B given in Eq.(3).

A schematic description of the whole algorithm is provided below, where ϵ_θ represents a tuning parameter used to update the generic parameter θ and \mathcal{U}_d denotes the discrete Uniform distribution.

- 1: **Initialization:** set $m = 0$ and specify parameters starting values;
- 2: **while** $m < M$ **do**
- 3: set $m = m + 1$;
- 4: draw $A' \sim \mathcal{D}(\epsilon_A A_1^{(m-1)}, \dots, \epsilon_A A_k^{(m-1)})$; ▷ update A
- 5: calculate Metropolis-Hastings' acceptance probability R
- 6: draw $u \sim \mathcal{U}(0, 1)$;
- 7: **if** $u \leq \min\{1, R\}$ **then** $A^{(m)} = A'$ **else** $A^{(m)} = A^{(m-1)}$ **end if**
- 8: **for** $j = 1, \dots, k^{(m-1)}$ **do** ▷ update τ
- 9: draw $\tau'_j \sim \mathcal{N}(\tau_j^{(m-1)}, \epsilon_\tau)$;
- 10: **if** $\tau'_j \notin (0; \tau_{\max})$ **then go to 9**
- 11: **end for**
- 12: calculate Metropolis-Hastings' acceptance probability R ;
- 13: draw $u \sim \mathcal{U}(0, 1)$;
- 14: **if** $u \leq \min\{1, R\}$ **then** $\tau^{(m)} = \tau'$ **else** $\tau^{(m)} = \tau^{(m-1)}$ **end if**
- 15: **for** $j = 1, \dots, k^{(m-1)}$ **do** ▷ update β
- 16: draw $u \sim \mathcal{U}(0, 1)$;
- 17: **if** $u \leq \zeta$ **then** draw $\beta'_j \sim \mathcal{B}(\kappa, \psi)$ **else** $\beta'_j = 1$ **end if**
- 18: **end for**
- 19: calculate Metropolis-Hastings' acceptance probability R ;
- 20: draw $u \sim \mathcal{U}(0, 1)$;
- 21: **if** $u \leq \min\{1, R\}$ **then** $\beta^{(m)} = \beta'$ **else** $\beta^{(m)} = \beta^{(m-1)}$ **end if**
- 22: draw $u \sim \mathcal{U}(0, 1)$; ▷ update γ
- 23: **if** $u \leq \xi$ **then** draw $\gamma' \sim \mathcal{B}(\varphi, \rho)$ **else** $\gamma' = 1$ **end if**
- 24: calculate Metropolis-Hastings' acceptance probability R ;
- 25: draw $u \sim \mathcal{U}(0, 1)$;
- 26: **if** $u \leq \min\{1, R\}$ **then** $\gamma^{(m)} = \gamma'$ **else** $\gamma^{(m)} = \gamma^{(m-1)}$ **end if**
- 27: draw $(\nu^{(m)})^{-1} \sim \mathcal{G} \left(\iota + \frac{n}{2}, \varsigma + \frac{1}{2} \sum_{i=1}^n \frac{\left(y_i - \gamma^{(m)} \sum_{j=1}^k A_j^{(m)} \exp \left(- \left(\frac{t_i}{\tau_j^{(m)}} \right)^{\beta_j^{(m)}} \right) \right)^2}{\sigma_i^2} \right)$; ▷ update ν
- 28: draw $u \sim \mathcal{U}(0, 1)$; ▷ update k
- 29: **if** $u \leq b_{k^{(m-1)}}$ **then** ▷ try birth
- 30: set $k' = k^{(m-1)} + 1$ and draw $j' \sim \mathcal{U}_d(1, k')$;
- 31: draw $A'_{j'} \sim \mathcal{B}(1, k^{(m-1)})$ and let $A'_j = A_j^{(m)}(1 - A'_{j'})$, $\forall j \neq j'$;
- 32: draw $\tau'_{j'} \sim \mathcal{U}(1, \tau_{\max})$;

```

33:   draw  $u \sim \mathcal{U}(0, 1)$ ;
34:   if  $u \leq \zeta$  then draw  $\beta'_{j'} \sim \mathcal{B}(\kappa, \psi)$  else  $\beta'_{j'} = 1$  end if
35:   calculate RJ acceptance probability  $B$ ;
36:   draw  $u \sim \mathcal{U}(0, 1)$ ;
37:   if  $u \leq \min\{1, B\}$  then
38:      $k^{(m)} = k'$ ,  $A^{(m)} = A'$ ,  $\tau^{(m)} = \tau'$ ,  $\beta^{(m)} = \beta'$ ;
39:   else
40:      $k^{(m)} = k^{(m-1)}$ ;
41:   end if
42: else ▷ try death
43:   set  $k' = k^{(m-1)} - 1$  and draw  $j' \sim \mathcal{U}_d(1, k^{(m-1)})$ ;
44:   delete  $A_{j'}^{(m)}$  and let  $A'_j = A_j^{(m)} / (1 - A_{j'}^{(m)})$ ,  $\forall j \neq j'$ ;
45:   set  $\tau' = \tau^{(m)}$  and  $\beta' = \beta^{(m)}$ ;
46:   delete  $\tau'_{j'}$  and  $\beta'_{j'}$ ;
47:   calculate RJ acceptance probability  $D$ ;
48:   draw  $u \sim \mathcal{U}(0, 1)$ ;
49:   if  $u \leq \min\{1, D\}$  then
50:      $k^{(m)} = k'$ ,  $A^{(m)} = A'$ ,  $\tau^{(m)} = \tau'$ ,  $\beta^{(m)} = \beta'$ ;
51:   else
52:      $k^{(m)} = k^{(m-1)}$ ;
53:   end if
54: end if
55: end while

```

Notice that, in the algorithm above, the proposal distributions used to propose new values of β and γ (lines 17 and 23, respectively) are simply the prior distributions of these parameters. This simplifies the calculation of the acceptance probability in Eq. (1), which reduces to the likelihood ratio.

In the case of PEG AuNP data, the algorithm used is a straightforward modification of the one presented above.

¹L. Tierney, Ann. Stat. **22**, 1701 (1994).